

Shear strength of the Zn–Sn high-temperature lead-free solders

R. Mahmudi · M. Eslami

Received: 16 November 2010/Accepted: 13 December 2010/Published online: 28 December 2010
© Springer Science+Business Media, LLC 2010

Abstract This study examines the shear strength behavior of the high-temperature Zn–20 wt% Sn, Zn–30 wt% Sn, and Zn–40 wt% Sn solders in the temperature range of 298–425 K. The results showed that increasing the Sn content of the alloys decreases both shear yield stress (SYS) and ultimate shear strength (USS) at all test temperatures. This can be attributed to the higher volume fraction of the softer β -Sn matrix and the eutectic α -Zn + β -Sn structure, which replaces the colonies of the harder α -Zn phase in the microstructure. The high shear strength of these high temperature solder alloys makes them suitable for application in harsh environments.

1 Introduction

Recent restrictions on the use of lead have stimulated a great deal of interest to research work to explore the possibility of developing suitable substitutes for the Sn–Pb solder alloys [1, 2]. Accordingly, many lead-free Sn-based alloy systems with different alloying elements such as; Ag, Cu, Zn, Bi, and Ni have been developed. The main criterion in the design of these new materials is a low melting point and good wettability, as prerequisites for an easy and inexpensive joining process. These Sn-based solders are primarily considered for intermediate-temperature applications, due to their relatively low melting range [3, 4]. For high-temperature applications, various lead-free solders such as Au–Sn, Bi–Ag, and Zn–Al based alloys have been proposed to replace the commonly used Pb–Sn alloys

containing 85 wt% to 97 wt% Pb [5]. However, high cost, formation of massive intermetallic compounds (IMC), and brittleness are known as typical disadvantages of these lead-free materials [3, 4].

To address these drawbacks, the new Zn–xSn alloys ($x = 20, 30, and 40 wt%) have recently been proposed as high-temperature lead-free solders [6]. It has been reported that these alloys have a sufficiently high melting temperature (i.e., liquidus temperature) and do not form any IMCs [7]. Kim et al. [8] have studied the potentials of Zn–Sn alloys as high-temperature solders for die attachment. They further examined the microstructures of the joint interface, stability during multiple reflow, shear strength of Cu/solder/Cu joint, and thermal conductivity of these alloys. In another work, Kim et al. [9] investigated the interfacial reactions of Si die-attached joints with Zn–Sn solders and found that a sound die-attachment on a Cu substrate could be achieved with no IMC phase in the Zn–Sn solder layer.$

Due to the potentially high service temperatures, strength of solder materials and its retention at elevated temperatures is of great interest. The mechanical properties of different intermediate-temperature solder alloys have been widely studied. On the other hand, the strength studies of the high-temperature lead-free solders are mainly confined to those obtained by the conventional tensile test [7, 10, 11] and shear test [6] of the Cu/solder/Cu joints at room temperature. The high-temperature performance of the Zn–Sn solder joints has been studied by the shear testing of the joints made on different substrates [12]. Recently, the study of impression creep behavior of the Zn–Sn alloys has shown that creep resistance deteriorates as the Sn content of the alloy increases [13]. Thus, the high-temperature strength of the bulk Zn–Sn solders has not been studied before and would be attempted in this investigation. This has been achieved using shear punch testing (SPT) technique which has been used in the

R. Mahmudi (✉) · M. Eslami
School of Metallurgical and Materials Engineering,
University of Tehran, Tehran, Iran
e-mail: mahmudi@ut.ac.ir

strength study of different engineering materials. There are many reports in the literature indicating that the SPT is an efficient method being capable of producing strength data which are well correlated with those found by the conventional tensile tests [14, 15]. Although this method has been primarily employed for testing thin wrought materials, it has been recently used for evaluating mechanical behavior of some cast alloys at both room [16, 17] and high temperature [18, 19]. This method can be particularly advantageous when the material is only available as small test pieces or there are difficulties with the machining of samples made of very soft materials such as solder alloys.

2 Experimental procedure

2.1 Materials and processing

The materials used were Zn–20 wt% Sn, Zn–30 wt% Sn, and Zn–40 wt% Sn alloys. They were prepared from high purity (99.97%) tin and zinc, melted in a graphite crucible at 450 °C in an electrical furnace under an inert argon atmosphere, and cast into 16-mm diameter bars. The cast bars were cut into 5-mm and 1-mm thick slices using an electrodischarge wire cut machine. The thicker slices were used for microstructural analysis, and the thinner ones were used for the assessment of mechanical properties. Scanning electron microscopy (SEM) was employed to examine the microstructure of the materials. The specimens were polished with 0.3-μm diamond paste, followed by polishing on an abrasive-free microcloth. Etching was carried out using a 20 g CrO₃, 1.5 g Na₂SO₄, and 100 mL H₂O at room temperature.

2.2 Shear punch test

The strength of the materials was assessed by the shear punch testing. The 1-mm thick slices of the materials were ground to a thickness of about 0.7 mm, from which disks of 15 mm in diameter were punched for the SPT. A shear punch fixture with a 3.175 mm diameter flat cylindrical punch and 3.225 mm diameter receiving-hole was used for this experiment. Shear punch tests were performed in the temperature range of 298–425 K using a screw driven SANTAM universal testing system equipped with a three-zone split furnace. After locating the specimen in the fixture, the assembly of the specimen and SPT fixture were accommodated by the split furnace. Then, the assembly was heated to the test temperature and held for 20 min to establish thermal equilibrium in the testing arrangement before the specimen was deformed by the punch. Tests were run with a load cell of 20 kN capacity and at a constant cross-head speed of 0.25 mm/min. After application

of the load, the applied load P was measured automatically as a function of punch displacement; the data were acquired by a computer so as to determine the shear stress of the tested materials using the relationship

$$\tau = \frac{P}{\pi dt} \quad (1)$$

where P is the punch load, t is the specimen thickness and d is the average of the punch and die diameters. Two different samples were tested for each condition and the variation in the measured ultimate shear strength values was small.

3 Results and discussion

The shear deformation behavior of all three materials was investigated by SPT. Although all SPT specimens had similar thicknesses in the range of 0.70–0.75 mm, the punch displacement was normalized to the specimen initial thickness in order to eliminate gage effects. Using Eq. (1), the punching load was converted to shear stress and plotted against the normalized displacement, as shown in Fig. 1a–c for all materials tested at different temperatures in the range of 298–425 K. As can be seen, similar to tensile stress–strain curves, each of the individual curves exhibits a linear part, after which a deviation from linearity is observed. Further loading of the samples results in the load-instability at which a maximum is observed in the stress-displacement curves. The deviation point is taken as the shear yield stress (SYS) and the stress corresponding to the maximum point is referred to as the ultimate shear strength (USS), as exhibited in Fig. 2.

Concerning the reproducibility of the SPT data, especially for the cast materials, care must be taken to consider the impact of the comparable sizes of the punch and defects, from one side, and inhomogeneity of the microstructural constituents from the other side. This is likely to cause significant scatter, depending on where the punching is made, and how many particles, grains, and other constituents contribute to the obtained load–displacement data. The same is true for the microstructural inhomogeneities and defects which may be located beneath the punch, affecting the materials resistance to punching. In the present work, however, at least two separate samples were tested and the obtained flow curves were very similar in terms of SYS and USS values, as shown for the test temperature of 325 K in Fig. 3. This may imply that, due to the relatively high solidification rate, a refined microstructure has been resulted, and hence the SPT data exhibit a high level of reliability. Therefore, SPT can be considered as a useful tool for investigating the mechanical properties of the present soft solder alloys at different temperatures.

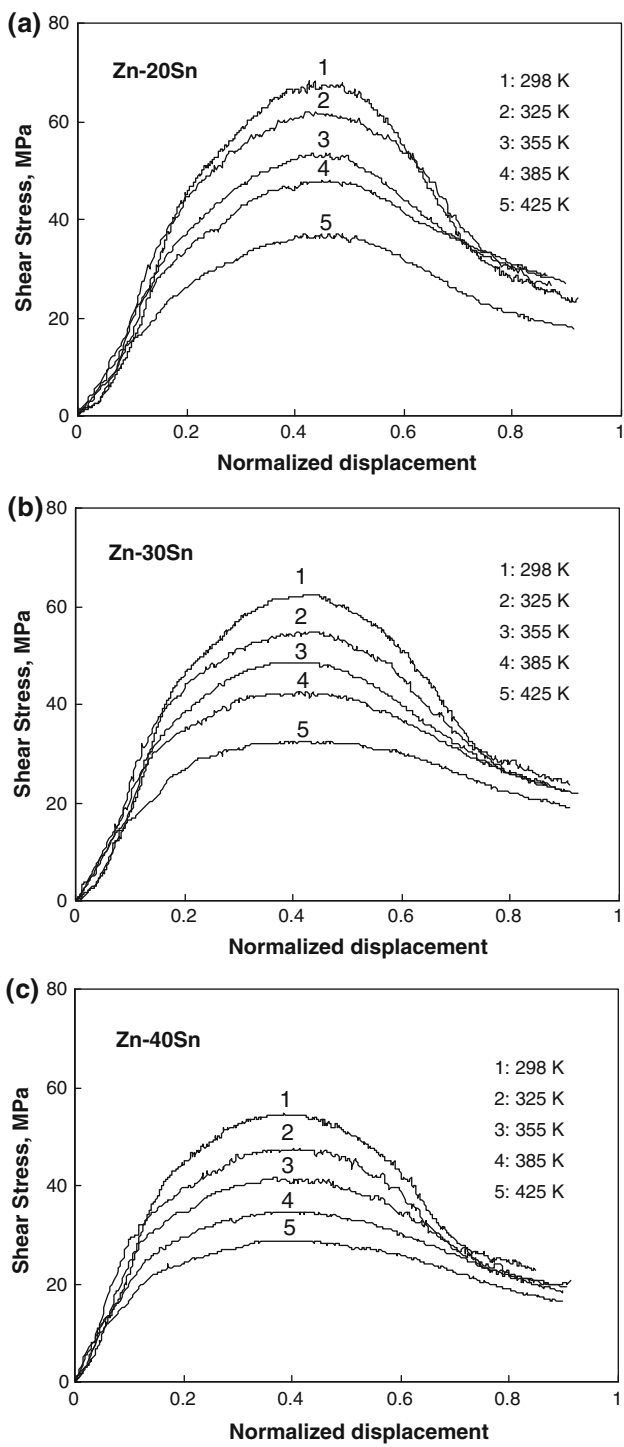


Fig. 1 Shear stress-normalized displacement curves at various temperatures for **a** Zn-20Sn, **b** Zn-30Sn, and **c** Zn-40Sn

In all test conditions studied in this work, increasing the test temperature from 298 to 425 K results in lower SYS and USS values. To have an overall view on the variation of strength with temperature, the SYS and USS data are summarized in Fig. 4a and b, respectively. The results indicate that as the Sn content of the alloys increases, both

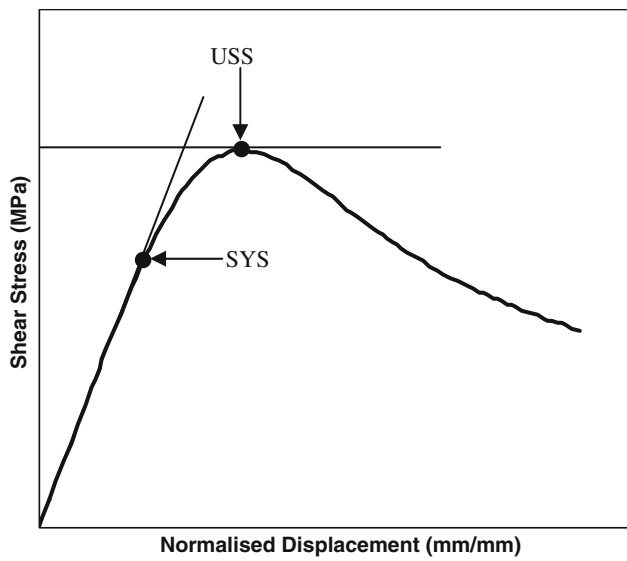


Fig. 2 Illustration of the method used for determination of ultimate shear strength (USS) and shear yield stress (SYS)

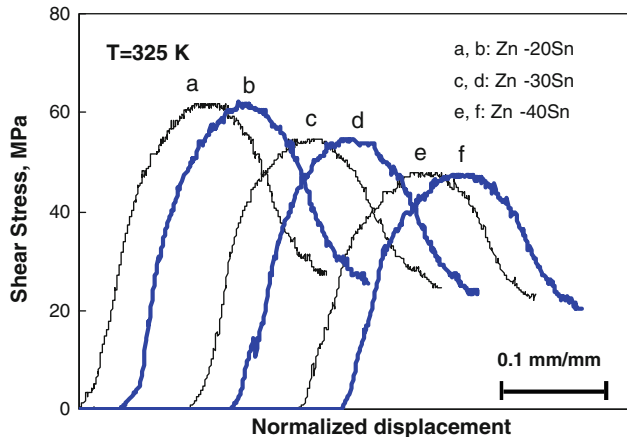


Fig. 3 Shear stress-normalized displacement curves, showing the reproducibility of the results obtained at 325 K for all three tested materials

SYS and USS values decrease at all test temperatures. The highest strength belongs to the Zn-20Sn alloy and the lowest to the Zn-40Sn alloy. It is worth noting that the same trend has been reported for the impression creep resistance of the same alloys [13]. Unfortunately, the literature lacks any data for the shear strength for the bulk of high Pb alloys to be compared with the shear strengths obtained for the Zn-Sn solders in this work. However, the reported 14 and 10 MPa tensile yield stresses of Pb-5Sn obtained, respectively at 298 and 373 K [10], are even much lower than the corresponding shear yield stresses of 30 and 20 MPa, found for the Zn-Sn alloys in the present work.

The observed differences in the flow behavior of the tested materials can be attributed to their respective

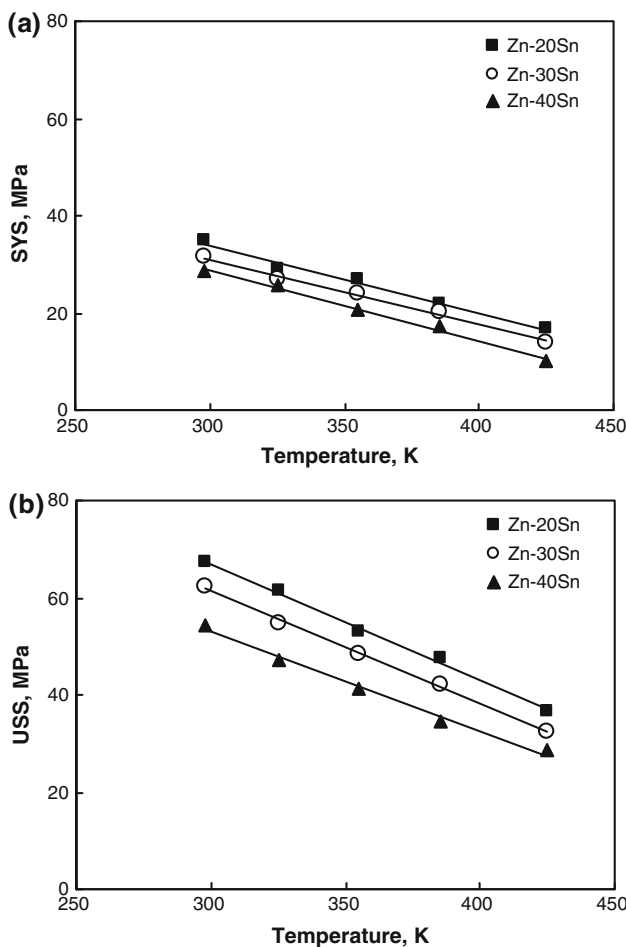


Fig. 4 Comparison of **a** SYS, and **b** USS of the materials tested at different temperatures

microstructures. SEM micrographs of the tested materials, shown in Fig. 5, indicate that the dark phase is primary α -Zn and the bright phase is eutectic α -Zn + β -Sn. The isolated patches of primary α -Zn are surrounded by the eutectic α -Zn + β -Sn structure. It can be observed that the volume fraction of the eutectic structure increases and that of the α -Zn phase decreases as the Sn content of the alloy increases. A higher-magnification view of this structure, shown in Fig. 6, indicates that some sparse eutectic α -Zn particles are dispersed in the β -Sn matrix. Qualitative analysis of the primary Zn phase and the eutectic structure determined by EDX has indicated that Zn is the main constituent (99.6 wt%) of the dark phase while the eutectic structure is composed of about 93.8 wt% Sn and 6.2 wt% Zn [13].

The higher shear strength of the Zn–20Sn alloy can be attributed to its lower Sn content, which results in a lower volume fraction of the eutectic structure. Similar to the strengthening of composites, the overall deformation resistance of the material depends on the volume fractions and strength of the alloy constituents, based on the rule of

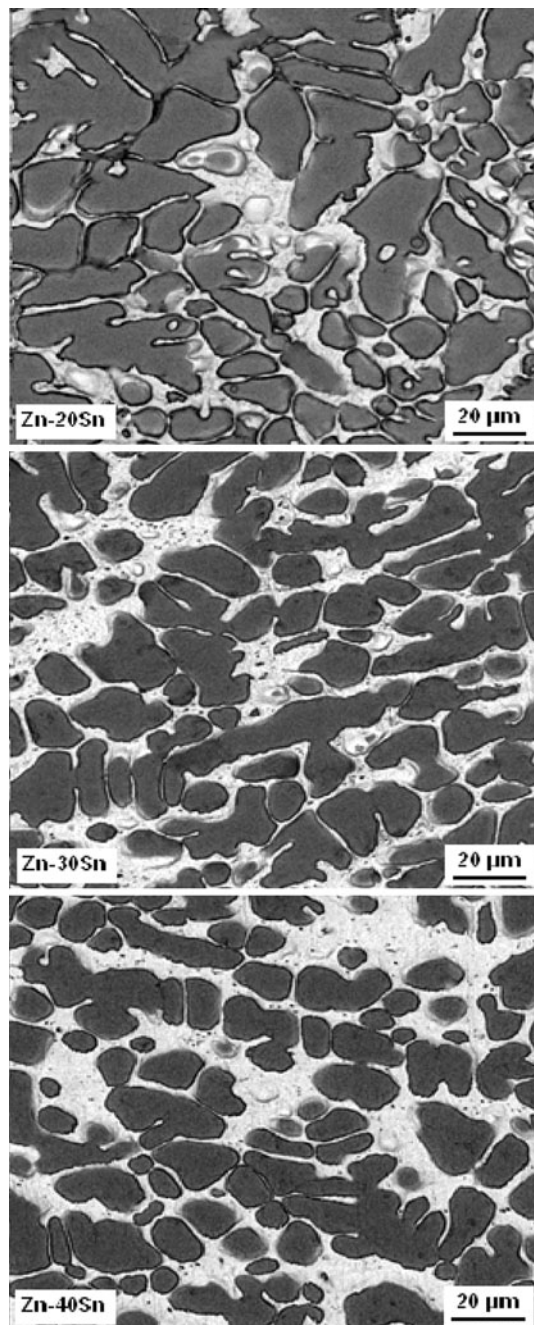


Fig. 5 SEM micrographs of the tested materials showing the general views of the microstructural constituents

mixtures [20]. It is well known that microhardness testing is a useful technique to evaluate the mechanical properties of different phases of the microstructure. The microhardness of α -Zn and the eutectic structure was measured using a very low load of 5 mN. As depicted in Fig. 6, the smaller size of the indentation on α -Zn is indicative of a harder phase with a hardness value of about 16, while the larger indentation size on the softer eutectic structure corresponds to a hardness of about 10. Figure 6 also shows that the soft

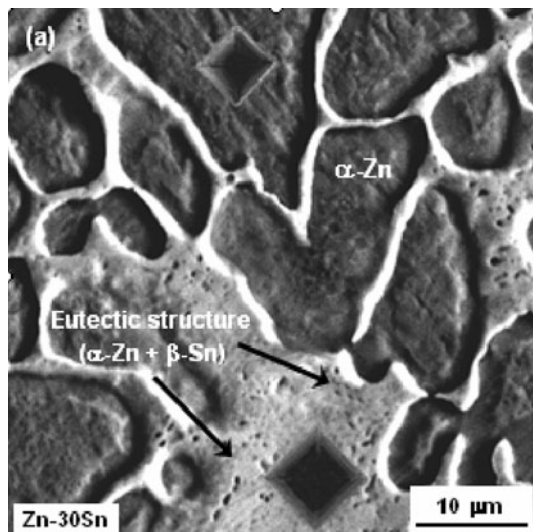


Fig. 6 SEM image of the Zn–30Sn showing the Vickers hardness indentations on the dark $\alpha\text{-Zn}$ phase and the bright eutectic $\alpha\text{-Zn} + \beta\text{-Sn}$ structure

eutectic structure is continuous and acts as a matrix which encompasses the harder $\alpha\text{-Zn}$ phase. Therefore, it can be inferred that, as the Zn content of the alloy increases, the volume fraction of the weaker $\beta\text{-Sn}$ decreases and the strength increases substantially. It is generally accepted that eutectics are often the hardest component in a phase diagram because of dispersion or phase-boundary strengthening. However, the phase boundaries, which provide hardening at low temperatures, can also give rise to sliding at high temperatures, and cause softening. The structure of the eutectic, viewed at high magnification, shows that it is divorced rather than lamellar. Concerning the strengthening effects of phase boundaries, it is to be noted that it was not possible to check their behavior at low temperatures, because room temperature is sufficiently high for them. Furthermore, in short-time microhardness tests it is unlikely that any significant sliding occurs. It is therefore, inferred that the volume fraction of the harder $\alpha\text{-Zn}$ phase is controlling the overall shear strength of the alloys.

4 Conclusions

The high-temperature shear strength of Zn–20Sn, Zn–30Sn, and Zn–40Sn solder alloys were tested by the shear punch

testing method in the temperature range of 298–425 K. According to the obtained shear strength data, increasing the Sn content of the alloys resulted in lower shear strengths at all test temperatures. This can be attributed to the microstructure of the alloys, which contains soft Sn-rich matrix encompassing the harder Zn phase. Such structures behave similarly to composites, the deformation resistance of which is controlled by both the volume fraction and strength of each phase. The high shear strength of these Zn–Sn solders makes them suitable candidates to be used instead of high Pb alloys in high temperature applications.

References

1. A.R. Geranmayeh, R. Mahmudi, J. Elec. Mater **34**, 1002–1009 (2005)
2. R. Mahmudi, A.R. Geranmayeh, M. Bakherad, M. Allami, Mater. Sci. Eng. A **457**, 173–179 (2007)
3. K. Saganuma, Curr. Opin. Solid State Mater. Sci **5**, 55–64 (2001)
4. K.S. Kim, S.H. Huh, K. Saganuma, Microelectron. Reliab **43**, 259–267 (2003)
5. L.S. Kim, C.H. Yu, N.H. Kim, N.K. Kim, H.J. Chang, E.G. Chang, Microelectron. Reliab **43**, 757–763 (2003)
6. K. Saganuma, Japan patent 2004-237375 (26 Aug 2004)
7. J.E. Lee, K.S. Kim, K. Saganuma, M. Inoue, G. Izuta, Mater. Trans **48**, 584–593 (2007)
8. S. Kim, K.S. Kim, S.S. Kim, K. Saganuma, J. Electron. Mater **38**, 266–272 (2009)
9. S. Kim, K.S. Kim, K. Saganuma, G. Izuta, J. Electron. Mater **38**, 873–883 (2009)
10. K. Saganuma, S.J. Kim, K.S. Kim, JOM **61**(1), 64–71 (2009)
11. J.E. Lee, K.S. Kim, K. Saganuma, J. Takenaka, K. Hagio, Mater. Trans **46**, 2413–2418 (2005)
12. T. Takahashi, S. Komatsu, H. Nishikawa, T. Takemoto, J. Electron. Mater **39**, 1241–1247 (2010)
13. R. Mahmudi, M. Eslami, J. Electron. Mater **39**, 2495–2502 (2010)
14. R.K. Guduru, K.A. Darling, R. Kishore, R.O. Scattergood, C.C. Koch, K.L. Murty, Mater. Sci. Eng. A **395**, 307–314 (2005)
15. R.K. Guduru, A.V. Nagasekhar, R.O. Scattergood, C.C. Koch, K.L. Murty, Metall. Mater. Trans **37A**, 1477–1483 (2006)
16. B. Kondori, R. Mahmudi, Mater. Sci. Eng. A **527**, 2014–2021 (2010)
17. R. Alizadeh, R. Mahmudi, Mater. Sci. Eng. A **527**, 5312–5317 (2010)
18. R. Alizadeh, R. Mahmudi, Mater. Sci. Eng. A **527**, 3975–3983 (2010)
19. G. Nayyeri, R. Mahmudi, F. Salehi, Mater. Sci. Eng. A **527**, 5353–5359 (2010)
20. M. Kangooie, R. Mahmudi, A.R. Geranmayeh, J. Electron. Mater **39**, 215–222 (2010)